

Potency and Selectivity Optimization of Tryptophanol-Derived Oxazoloisoindolinones: Novel p53 Activators in Human Colorectal Cancer

Valentina Barcherini,^[a] Joana Almeida,^[b] Elizabeth A. Lopes,^[a] Mi Wang,^[c]
Diogo Magalhães e Silva,^[a] Mattia Mori,^[d] Shaomeng Wang,^[e] Lucília Saraiva,^{*,[b]} and
Maria M. M. Santos^{*,[a]}

To search for novel p53 activators, four series of novel (*S*- and (*R*)-tryptophanol-derived oxazoloisoindolinones were synthesized in a straightforward manner and their antiproliferative activity was evaluated in the human colorectal cancer HCT116 cell line. Structural optimization of the hit compound SLMP53-1 led to the identification of a (*R*)-tryptophanol-derived isoindolinone that was found to be six-fold more active, with increased selectivity for HCT116 cells with p53 and with low

toxicity in normal cells. Binding studies with MDM2 showed that the antiproliferative activity of tryptophanol-derived isoindolinones does not involve inhibition of the main negative regulator of the p53 protein. Molecular docking simulations showed that although these molecules establish hydrophobic interactions with MDM2, they do not possess the required features to bind MDM2.

Introduction

Colorectal cancer (CRC) represents the third most common malignancy worldwide and the fourth cause of cancer death, with 1.8 million new cases and 881.000 deaths reported in 2018.^[1,2] Thanks to the latest progresses in early stage identification of the disease and improvements in CRC treatment, the overall incidence of colon cancer has decreased in high-developed countries.^[3] Nevertheless, the incidence of CRC in individuals younger than 50 years has increased to 2%. In fact, it has been predicted that by 2030, the incidence of colon and rectal cancers could soar by 90% and 124%, respectively, for patients with age ranging from 20 to 34 years old.^[4]

Development of targeted therapies has led to promising advances in cancer treatment^[5] and one of the most promising therapeutic targets is the tumor suppressor protein p53, which is inactivated in most human cancers and is found mutated in

50% of malignancies.^[6–9] It is reported that p53 mutation develops in about 40–50% of CRC and patients with mutated p53 gene possibly gain multidrug resistance, leading to therapy failure.^[10,11]

p53 plays a crucial role in cellular homeostasis, actively regulating critical processes such as cell-cycle arrest, DNA repair and apoptosis.^[12,13] p53 has also a significant role in cell differentiation, autophagy, senescence, angiogenesis, programmed cell death and metabolism.^[14–16] In 50% of cancer malignancies wild-type p53 is inhibited by overexpression of endogenous negative regulators, such as murine double minute-2 (MDM2, also called HDM2 in humans) and murine double minute-X (MDMX or MDM4 and known as HDMX in humans).^[17] In the remaining 50% of human cancers, p53 is inactivated by missense mutations mainly located in its DNA-binding domain, leading to loss of its wild-type tumor suppressor function.^[18] Therefore, most p53-based cancer therapies are based on p53 pharmacological reactivation.^[19] To date, most of these strategies were focused on the inhibition of its main negative regulator MDM2,^[17] or on the pharmacological restoration of wild-type-like activity to mutant p53 forms.^[20–23]

In the past 20 years, several chemical libraries were developed with the aim of inhibiting MDM2 and p53 interaction and currently only one small molecule, HDM201, has undertaken clinical development for colorectal cancer in combination therapies.^[24,25]

In this area of research, we have identified several small molecules that are able to activate the p53 pathway.^[26–29] Among them, the enantiopure tryptophanol-derived oxazoloisoindolinone SLMP53-1 (**1**) was identified as a promising hit with p53-dependent antiproliferative activity *in vitro* and *in vivo* in human tumor cells from a phenotypic screening of an in-house amino alcohol-derived library (Figure 1).^[30]

[a] V. Barcherini, E. A. Lopes, D. Magalhães e Silva, Dr. M. M. M. Santos
Department of Therapeutic and Pharmaceutical Chemistry, University of
Lisbon


Av. Prof. Gama Pinto, 1649-003 Lisboa (Portugal)
E-mail: mariasantos@ff.ulisboa.pt

[b] J. Almeida, Dr. L. Saraiva
Department of Biological Sciences, University of Porto
Rua de Jorge Viterbo Ferreira 228, 4050-313 Porto (Portugal)
E-mail: lucilia.saraiva@ff.up.pt

[c] Dr. M. Wang
Rogel Cancer Center, Medical School
University of Michigan, Ann Arbor, MI 48109 (USA)

[d] Dr. M. Mori
Department of Biotechnology, Chemistry and Pharmacy
University of Siena, via Aldo Moro 2, 53100 Siena (Italy)

[e] Dr. S. Wang
Rogel Cancer Center, College of Pharmacy
University of Michigan, Ann Arbor, MI 48109 (USA)

 Supporting information for this article is available on the WWW under
<https://doi.org/10.1002/cmdc.202000522>

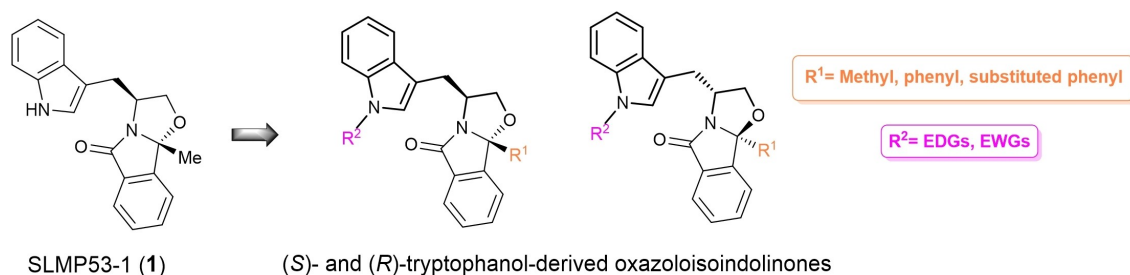


Figure 1. Strategy for the optimization of the p53 reactivator SLMP53-1 (1).

To investigate the structure-activity relationships (SARs) for this new chemical class of p53-reactivating drugs, the 9b-substituent of the oxazoloisindolinone moiety and the indole nitrogen were selected for modification leading to other promising p53 activators, two times more potent than SLMP53-1.^[31,32] Herein, we report the complete structure-activity study that led to these compounds, and further optimization leading to a derivative that is four times more potent than SLMP53-1 and more selective for HCT116 cells expressing p53 over the isogenic cells that do not express p53.

Results and Discussion

Approach and synthetic strategy

N-unsubstituted tryptophanol-derived oxazoloisindolinones 1 and 10, containing a methyl or a phenyl group in position 9b, were prepared by stereoselective cyclocondensation of (*S*)-tryptophanol and 2-substituted benzoic acids, with yields of 81% and 79%, respectively, as previously reported by our

group.^[33] The reactions were performed in toluene under reflux using a Dean-Stark apparatus.

The first compound set 2–9 was prepared varying the substituent at the indole nitrogen while retaining the methyl group in position 9b (Figure 2). Analogues 11–18 with a phenyl group instead of a methyl group in position 9b were also prepared to evaluate the impact of a bulkier hydrophobic aromatic group on the biological activity. Moreover, both electron-donating and lipophilic (methyl, ethyl, propyl and benzyl) and electron-withdrawing (acetyl, *tert*-butoxycarbonyl, benzoyl and tosyl) groups were tested to evaluate the effect on the activity of the *N*-substituent size and electronegativity.

The *N*-indole protected tryptophanol-derived isindolinones were easily prepared with yields ranging from 68–96%. Compounds 2–4 and 11–13 were synthesized by reaction of the corresponding unprotected tryptophanol-derived isindolinones with alkyl halides in the presence of sodium hydride. Tryptophanol-derived oxazoloisindolinones 5 and 14 were synthesized by reaction of the corresponding unprotected tryptophanol-derived isindolinones with acetic anhydride. Compounds 6 and 15 were synthesized by reacting the unprotected tryptophanol-derived isindolinones with *tert*-

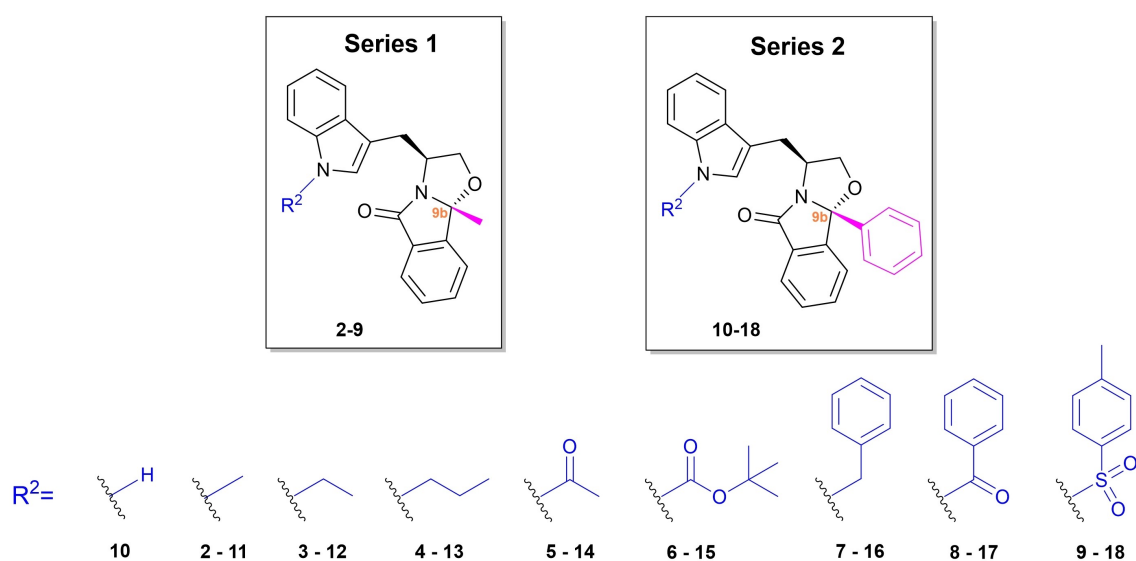


Figure 2. Structures of *N*-indole substituted derivatives 2–9 and 11–18 and *N*-indole unsubstituted derivative 10.

butoxycarbonyl anhydride in the presence of triethylamine and *N,N*-dimethylpyridin-4-amine at room temperature. Benzyl bromide, benzoyl bromide and *p*-toluenesulfonyl chloride were used to access analogues **7/16**, **8/17**, and **9/18**, respectively.

To study the effect of introducing substituents at the *9b*-phenyl group, compounds **19–23** (Figure 3) were prepared by cyclocondensation reaction of (*S*)-tryptophanol with substituted benzoyl benzoic acids. Tryptophanol-derived oxazoloisindolinones **19–20** and **22–23** with a fluorine, a chlorine, a methoxy, and a methyl group, respectively, at the *para* position were obtained in yields of 55–82%. Additionally, compound **21**, with a chlorine atom at the *para* position and a nitro group at the *meta* position was obtained from reaction of (*S*)-tryptophanol with 2-(4-chloro-3-nitrobenzoyl)benzoic acid. In this reaction,

compound **21** was isolated in 45% yield together with a minor quantity of the cyclized product (6% yield) (Scheme 1).

The effect of the stereochemistry on the activity was also evaluated by synthesizing compounds **24–34** (*R*)-tryptophanol-derived enantiomers of the most active compounds in HCT116 p53^{+/+} containing a phenyl group at position 9b; see Figure 4).

Except for the cyclocondensation reaction of tryptophanol with 2-(4-chloro-3-nitrobenzoyl)benzoic acid, in all reactions, the formation of only one diastereoisomer was observed by TLC, ¹H- and ¹³C-NMR spectroscopies. The absolute configuration of the stereogenic center in position 9b of compounds **2–34** was determined by ¹³C-NMR spectroscopy. For compounds **2–9** and **10–34** the chemical shift of C-9b appears between 98.9–99.1 ppm and 99.9–101.3 ppm, respectively. These chemical shifts are in agreement with the ones reported for SLMP53-

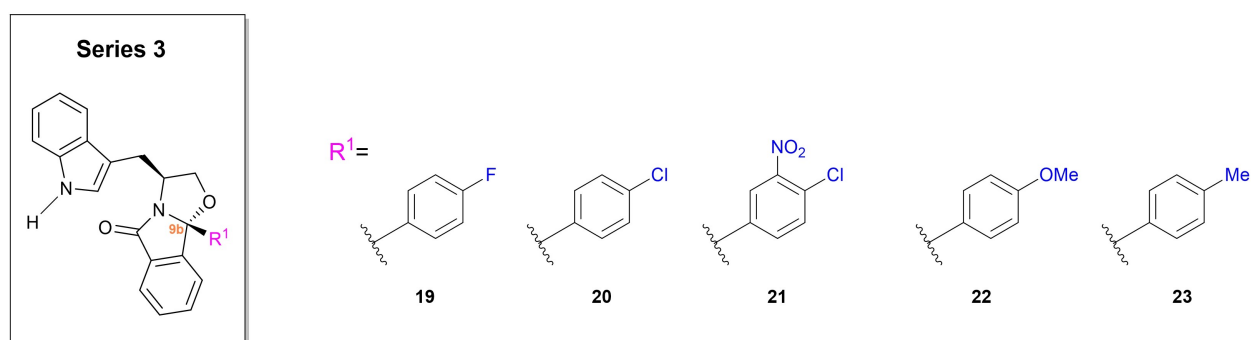
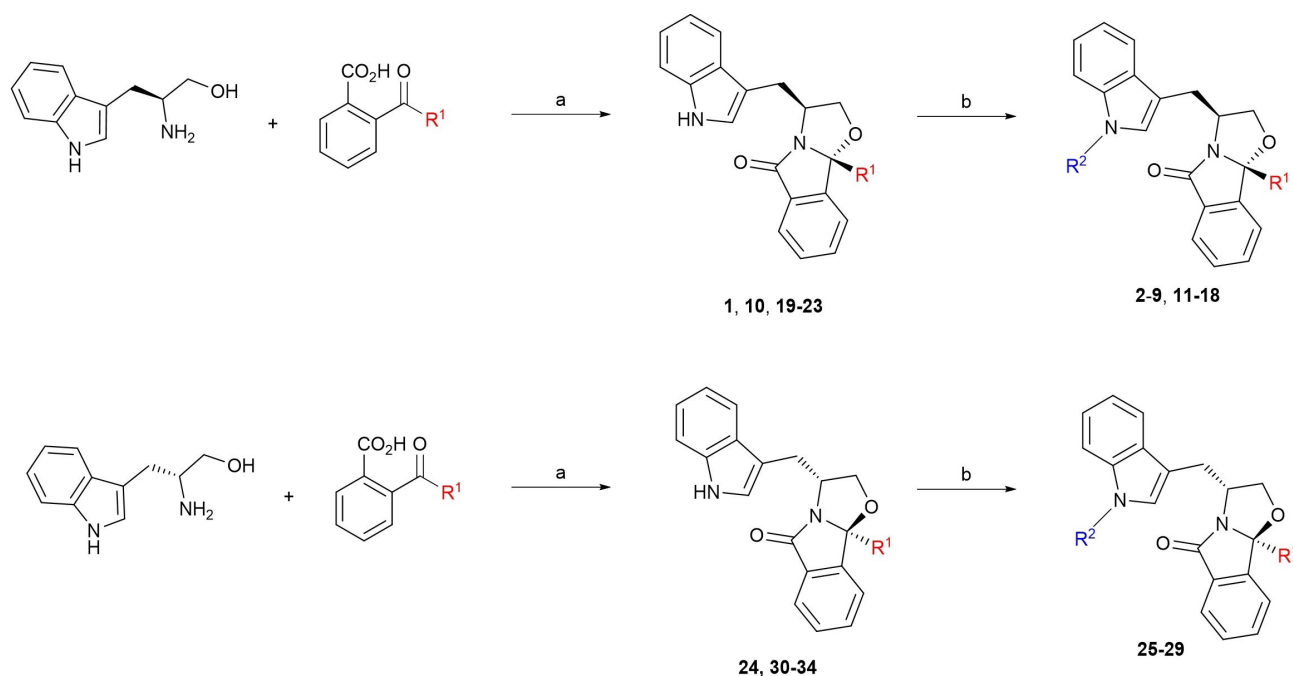


Figure 3. Structures of *9b*-Phenyl substituted analogues **19–23**.



Scheme 1. Synthetic route to prepare enantiomerically pure tryptophanol-derived isoindolinones: **1, 10, 19–24, 30–34**: (a) toluene, reflux. **2–3, 11–12, 25–26** (b): R₂I, NaH, DMF, rt. **4, 7, 13, 16, 27** (b): R₂Br, NaH, DMF, rt. **5, 14, 28** (b): (R₂)₂O, NaH, DMF, rt. **6, 15** (b): Et₃N, DMAP, (R₂)₂O, THF, rt. **8–9, 17–18, 29** (b): R₂Cl, NaH, DMF, rt.

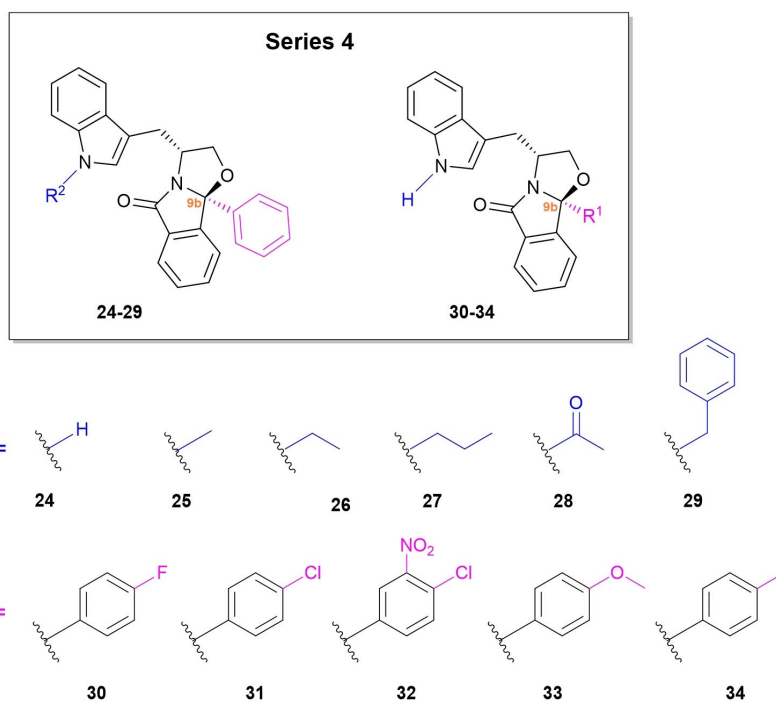


Figure 4. Structures of (*R*)-tryptophan-derived isoindolinones 24–34.

1,^[33] confirming the 3,9b-(*S,R*)-relationship for compounds 2–23, and 3,9b-(*R,S*)-relationship for compounds 24–34.^[30,32,34]

Structure-activity relationship studies

The antiproliferative effect of the compounds prepared in series 1–3 was evaluated in human colon adenocarcinoma HCT116 cell line (Figures 5 and 6). Most compounds displayed

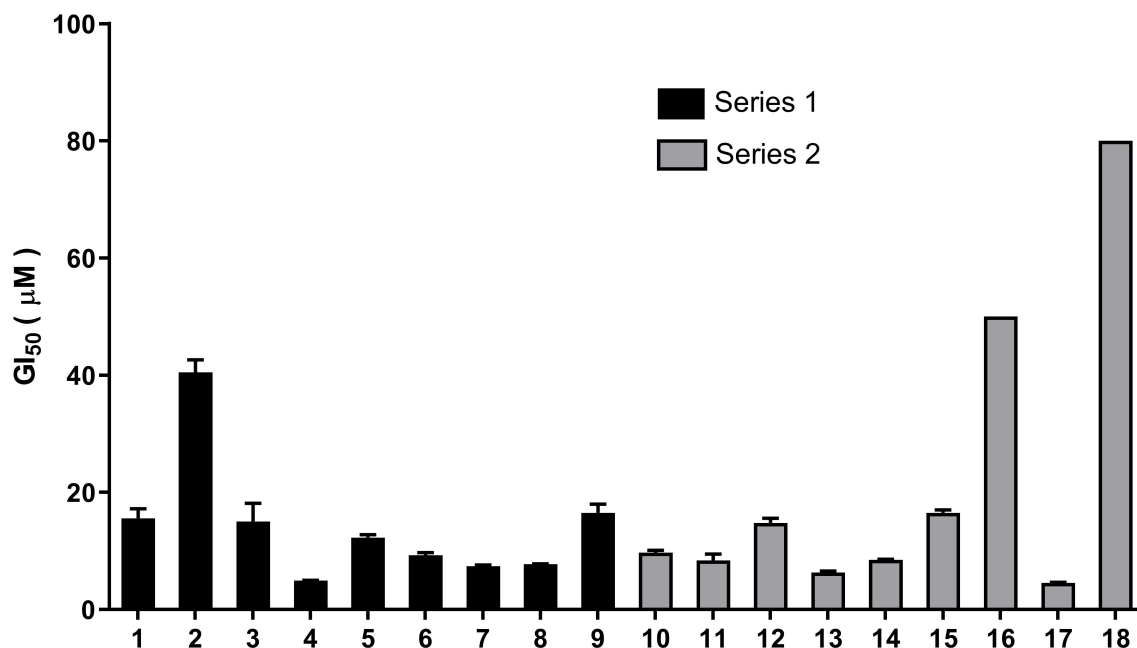


Figure 5. Tryptophan-derived isoindolinones 1–23 screened in HCT116 human colorectal carcinoma cells. Growth inhibitory effect was determined after 48 h treatment; growth obtained with control (DMSO) was set as 100%. Data are mean \pm SEM of 3–5 independent experiments.

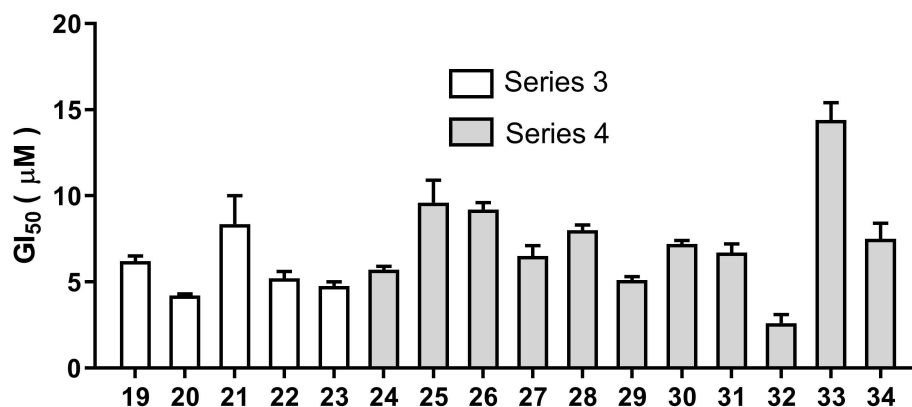


Figure 6. Tryptophanol-derived isoindolinones 24–32 screened in HCT116 human colorectal carcinoma cells. Growth inhibitory effect was determined after 48 h treatment; growth obtained with control (DMSO) was set as 100%. Data are mean \pm SEM of 3–5 independent experiments.

GI₅₀ lower than 20 μ M, with 25 compounds presenting a GI₅₀ lower than the hit compound 1 (Table 1).

For series 1, the introduction of a methyl (Me) at the *N*-indole (compound 2) led to loss of activity compared with the unprotected derivative 1. However, longer alkyl chains, such as ethyl (Et) or propyl (Pr), were well tolerated. Specifically, the introduction of an ethyl (compound 3) led to a derivative with almost the same potency of compound 1, while the introduction of a propyl (compound 4) led to a 3.1-fold increase on activity. The introduction of electron-withdrawing groups at the *N*-indole was also well tolerated. The presence of acetyl (Ac), *tert*-butyloxycarbonyl (Boc), benzyl (Bn) and benzoyl (Bz) substituents, led to more potent derivatives (compounds 5–8 versus compound 1). The presence of a tosyl (Ts), a bulkier electron-withdrawing group, led to a derivative (compound 9)

with almost the same activity as the hit compound. In the derivatives with a phenyl ring at position 9b (series 2), the introduction of a benzyl (Bn) or a tosyl (Ts) group at the *N*-indole, compounds 16 and 18, led to loss of activity compared with the hit compound 1 and the *N*-unprotected derivative 10. However, all other derivatives (compounds 11–15 and 17) were equally potent or more active than the hit compound. The most active compound in this series was compound 17, containing a benzoyl (Bz) substituent, being 3.4-fold more active than hit compound 1.

The introduction of different substituents (halogens, methoxy and methyl) at the 9b-phenyl group led to more active derivatives (compounds 19–23 versus the unsubstituted derivative 10). Of this series of compounds, the most active derivatives were compounds 20 and 23, with two substituents with similar van der Waals radii (chloro and methyl).^[35,36]

The antiproliferative effect in HCT116 cells was also assessed for the (*R*)-tryptophanol-derived isoindolinones 24–34 (Series 4, Figure 4), enantiomers of the most active (*S*)-tryptophanol analogues containing an aromatic group at position 9b.

All derivatives presented GI₅₀ equal or lower than GI₅₀ of hit compound 1 (SLMP53-1). When compared to the activities of pairs of enantiomers (Figure 6), for most derivatives, the activities of both enantiomers were very similar. However, this was not the case of (*R*)-tryptophanol derivatives 24, 26 and 32 which were more active than the correspondent (*S*)-tryptophanol enantiomers 10, 12 and 21, respectively. Specifically, the most active derivative was compound 32, with an unprotected *N*-indole and a disubstituted 9b-phenyl ring (chlorine and nitro substituents), which was 6-fold more active than the hit compound 1. Moreover, the presence of a methoxy or a methyl group at the *para* position of the 9b-phenyl ring (compounds 33 and 34) led to less potent compounds compared with the (*S*)-tryptophanol-derivatives (compounds 22 and 23).

Compound	HCT116 p53 ^{+/+} GI ₅₀ [μ M]	HCT116 p53 ^{-/-} GI ₅₀ [μ M]	SI ^a
1	15.5 \pm 1.6 ^[30]	34.0 \pm 3.5 ^[30]	2.2
10	9.7 \pm 0.4	9.7 \pm 0.3	1.0
11	8.4 \pm 1.1 ^[32]	17.7 \pm 2.3 ^[32]	2.1
13	6.35 \pm 0.2	7.0 \pm 1.1	1.1
14	8.5 \pm 0.1	9.5 \pm 1.5	1.1
17	4.55 \pm 0.1	3.8 \pm 0.3	0.8
19	6.2 \pm 0.3	7.4 \pm 0.1	1.2
20	4.2 \pm 0.1	4.8 \pm 0.3	1.1
21	8.35 \pm 1.65	8.95 \pm 0.75	1.1
22	5.2 \pm 0.4	5.6 \pm 0.7	1.1
23	4.75 \pm 0.05	6.3 \pm 0.4	1.3
24	5.7 \pm 0.2	7.0 \pm 0.5	1.2
25	9.6 \pm 1.3	16.7 \pm 1.9	1.7
26	9.2 \pm 0.4	7.3 \pm 0.9	0.8
27	6.5 \pm 0.6	10.0 \pm 1.3	1.5
28	8.0 \pm 0.3	5.4 \pm 0.4	0.7
29	5.1 \pm 0.2	3.6 \pm 0.2	0.7
30	7.2 \pm 0.2	9.9 \pm 1.3	1.4
31	6.7 \pm 0.5	9.0 \pm 0.4	1.3
32	2.6 \pm 0.5	8.6 \pm 0.4	3.3
34	7.5 \pm 0.9	10.2 \pm 0.8	1.4

[a] Selectivity index toward HCT116 p53^{+/+}, which is expressed by the ratio GI₅₀ HCT116 p53^{-/-}/GI₅₀ HCT116 p53^{+/+}.

Selectivity for the p53 pathway

To confirm the contribution to p53 activation in HCT116 p53^{+/+} cells, the compounds from series 2–4 with GI₅₀ values lower than 10 μM were also tested in HCT116 cells in which p53 has been knocked out (HCT116 p53^{-/-}). Several compounds revealed other mechanisms may contribute to compounds antiproliferative activity. However, (*R*)-tryptophan-derived oxazoloisoindolinones **11**, **25** and **32** were selective for p53^{+/+} HCT116 cells over cells with deleted p53. Compared with the hit compound **1**, compounds **11** and **25** presented higher antiproliferative activity but the selectivity for p53 was not increased. However, compound **32** showed 6-fold higher antiproliferative activity, as well as increased selectivity for p53, compared with the hit compound **1**. Moreover, as activator of wt p53, it became imperative to check the growth inhibitory activity of derivative **32** against normal cells. Compound **32** was tested in normal CCD-18Co colon cells. An IC₅₀ value in CCD-18Co cells (26.7 ± 1.8 μM), ten-fold higher than the obtained in HCT116 p53^{+/+} cells, indicated that, despite the expression of wt p53 in normal cells, compound **32** is selective towards cancer cells.

MDM2 inhibition studies

The p53-MDM2 protein-protein interaction consists of a steric complementary interface between the MDM2 cleft and the hydrophobic residues Phe19, Leu22, Trp23 and Leu26 of the α-helix of p53. The interaction between these two proteins is mainly established by van der Waals interactions, and it is complemented by a hydrogen bond between the p53 Phe19 backbone amide and the MDM2 Gln72 carbonyl group, and a hydrogen bond between the nitrogen of the p53 Trp23 and MDM2 Leu54 carbonyl group.^[19]

For efficient disruption of the p53-MDM2 protein-protein interaction, p53 activators that inhibit MDM2, should fill the four MDM2 pockets occupied by the Phe19, Leu22, Trp23, and Leu26 of p53.

Isoindolinone derivatives were previously reported to bind MDM2, promoting p53 activation.^[37–40] Using ligand-protein interaction NMR studies and ELISA binding assays it was shown that the isoindolinone moiety occupied the Trp23 pocket, and a *para*-substituted phenyl substituent occupied the Leu26 pocket.^[41] As isoindolinone ligands are known to act as MDM2 inhibitors, we decided to evaluate if the molecular target for the activation of p53 observed for compound **32** could be MDM2. We used a fluorescence polarization (FP) competitive binding assay, which showed that the compound was not able to compete with the fluorescent probe molecule that binds potently to MDM2. This finding was consistent with results obtained recently with compound **1** in cancer cell lines with mutated p53. In these cell lines, compound **1** was shown to activate wt p53 and restore wt-like function to mutp53 R280 K by directly binding to this protein.^[42]

To understand why tryptophan-derived isoindolinones do not inhibit MDM2 we performed molecular docking simulations

with compounds **1** and **32** using the crystallographic structure of MDM2 (PDB ID: 4WT2). Both compounds showed similar binding poses, with the indole moiety projected to the Leu26 pocket and the oxazolidine moiety projected to the Phe19 pocket (Figure 7). However, both compounds are unable to fill the four pockets of the MDM2 hydrophobic binding site. Specifically, compound **1** does not fill the Trp23 nor the Leu22 pockets, establishing only one hydrogen interaction with the carbonyl group of the backbone of His96. In compound **32**, although the 9b-phenyl group is projected to the Leu22 solvent-exposed pocket, the Trp23 pocket remains unfilled. Moreover, the nitro group establishes a hydrogen bond with the nitrogen of the Met6 residue. Although both tryptophan-derived oxazoloisoindolinones establish hydrophobic interactions with MDM2, these compounds do not possess important structural features of MDM2 inhibitors such as filling the Phe19, Leu22, Trp23, and Leu 26 pockets, establishing a hydrogen bond with Leu54 and having π-π stacking interaction with His96.

Conclusions

In this work, we describe the synthesis and structure-activity study of a chemical library of thirty-four enantiopure tryptophan-derived oxazoloisoindolinones as p53 activators. Optimization of the hit compound **1** (SLMP53-1) led to the development of compound **32**, with a GI₅₀ value of 2.6 μM in HCT116 p53^{+/+} cells, and increased selectivity for cells with p53 over those cells without p53. It was shown that the mechanism of action of compound **32** as p53 activator does not involve the inhibition of the p53 main negative regulator (MDM2). Further studies are ongoing to optimize the activity and selectivity of this compound, and to identify the alternative mechanism of action of compound **32** for p53 activation.

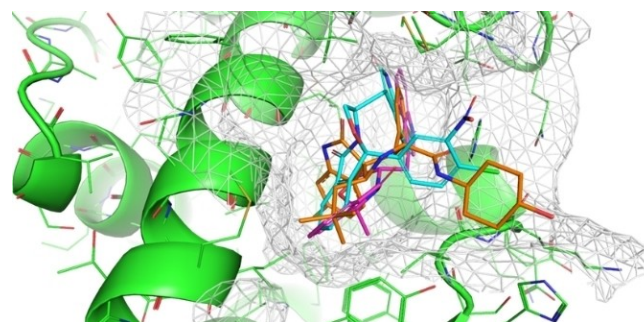


Figure 7. Docking poses of compounds **1** (pink sticks) and **32** (blue sticks) in MDM2 (green cartoon with a surface). Crystallographic structure of a known MDM2 inhibitor, SAR405838 (orange sticks), that fills Phe19, Leu22, Trp23, and Leu26 pockets and establishes two hydrogen bonds between the NH of the indole with Leu54 and the carbonyl group with His96, and a hydrophobic π-π stacking interaction between the phenyl ring and His96.

Experimental Section

Materials. Colon adenocarcinoma HCT116 cell lines expressing wt p53 (HCT116 p53^{+/+}) and its p53-null isogenic derivative (HCT116 p53^{-/-}) were provided by B. Vogelstein (The Johns Hopkins Kimmel Cancer Center, Baltimore, MD, USA). Normal CCD-18Co colon cells were purchased from American Type Culture Collection (ATCC, Manassas, VA, USA). Tumor cells were cultured in RPMI-1640 with UltraGlutamine (Lonza, VWR) and CCD-18Co cells in EMEM (Lonza, Ingrenor, Porto, Portugal), supplemented with 10% fetal bovine serum (FBS; Gibco, Alfacene) and maintained in a humidified incubator at 37 °C with 5% CO₂. All reagents were commercially available. (*R*)-tryptophan was synthesized by reduction of (*R*)-tryptophan with Lithium Aluminium hydride.^[43] Tryptophan-derived oxazoloisindolinones **1** and **7** were synthesized as previously reported.^[30,31] Thin-layer chromatography was performed on SiO₂ (Merck Silica Gel 60 F254 plates) and spots located by UV lamp. Flash column chromatography was performed using Merck Silica Gel (200–400 mesh). ¹H and ¹³C NMR spectra were recorded on a Bruker 300 MHz/54 mm Ultra-Shield Spectrometer (Wissensbourg, Bas-Rhin, France). ¹H nuclear magnetic resonance spectra were recorded at 300 MHz. ¹³C nuclear magnetic resonance spectra were recorded at 100 MHz. ¹H and ¹³C NMR chemical shifts are reported in parts per million (ppm, δ) referenced to the solvent used and the proton coupling constants *J* in Hertz (Hz). Multiplicities are given as: s (singlet), d (doublet), dd (double doublet), t (triplet), q (quartet) and m (multiplet). Spectra were assigned using appropriate COSY, DEPT, HMQC and HMBC sequences. Melting points were determined using a Kofler camera Bock monoscope M. Microanalysis was performed in a Flash 2000 CHNS–O Thermo-Scientific elemental analyzer, at Liquid Chromatography and Mass Spectrometry Laboratory, Faculty of Pharmacy of Lisbon University. Values are reported within $\pm 0.4\%$ of theoretical values. All compounds showed purity $\geq 90\%$ by LC-MS, performed in a Waters Alliance 2695 HPLC with a Waters SunFire C18 column (100 \times 2.1 mm, 5 μ m) at 35 °C, using as mobile phase a gradient from 95% solution A (Milli-Q water containing 0.5% formic acid (v/v)) to 95% solution B (acetonitrile) and employing a photodiode array detector to scan wavelength absorption from 210 to 600 nm. MS experiments were performed on Micromass[®] Quattro Micro triple quadrupole (Waters[®], Ireland) with an electrospray in positive ion mode (ESI+), ion source at 120 °C, capillary voltage of 3.0 kV and source voltage of 30 V, at the Liquid Chromatography and Mass Spectrometry Laboratory, Faculty of Pharmacy, University of Lisbon. Optical rotations were determined with P-200 high-accuracy digital polarimeter JASCO.

General procedure for the cyclocondensation reaction – To a stirred solution of (*R*)- or (*S*)-tryptophan (0.53 mmol, 1.0 equiv.) in toluene (5 mL), was added the appropriate oxo-acid (0.58 mmol, 1.1 equiv.). The mixture was heated at reflux under inert atmosphere using Dean-Stark conditions for 10–24 hours. At the end of the reaction the solvent was evaporated under reduced pressure, and the crude diluted in 15 mL of ethyl acetate and washed with 1 \times 15 mL of NaHCO₃ and then with 1 \times 15 mL of brine. The organic phase was dried over Na₂SO₄. After removal of volatiles under reduced pressure, purification via flash chromatography followed by recrystallization in ethyl acetate/*n*-hexane afforded the desired product.

(3*R*,9*B*5)-3-((1*H*-indol-3-yl)methyl)-9*b*-(4-chloro-3-nitrophenyl)-2,3-dihydrooxazolo[2,3-*a*]isindol-5(9*b*H)-one (32). Following the general procedure, starting from (*R*)-tryptophan (0.132 g, 0.693 mmol), toluene (7.5 mL) and 2-(4-chloro-3-nitrophenyl)benzoic acid (0.233 g, 0.762 mmol). Reaction time: 16.5 hours. Eluent for flash chromatography: ethyl acetate/*n*-hexane, 4:6. The product was obtained as a yellow light solid (0.141 g, 44.5%). Mp: 94–96 °C; $[\alpha]_D^{20} = -58.1^\circ$ (*c* = 0.43, CH₂Cl₂). ¹H NMR (300 MHz, CDCl₃) δ 8.03 (s,

1H, NH), 8.01 (d, *J* = 2.0 Hz, 1H, ArH), 7.86–7.80 (m, 1H, ArH), 7.55–7.48 (m, 3H, ArH), 7.38 (dd, *J* = 8.4, 2.1 Hz, 1H, ArH), 7.33–7.25 (m, 2H, ArH), 7.22–7.06 (m, 3H, ArH), 7.04 (s, 1H, ArH), 4.72 (m, 1H, H-3), 4.53 (dd, *J* = 8.7, 7.7 Hz, 1H, H-2), 4.09 (dd, *J* = 8.4, 6.9 Hz, 1H, H-2), 3.06 (dd, *J* = 14.9, 5.3 Hz, 1H, CH₂-indole), 2.89 (dd, *J* = 14.7, 8.0 Hz, 1H, CH₂-indole); ¹³C NMR (75 MHz, CDCl₃) δ 174.71 (C=O), 147.97 (Cq), 146.36 (Cq), 140.30 (Cq), 136.18 (Cq), 133.91 (ArCH), 132.06 (ArCH), 131.00 (Cq), 130.91 (ArCH), 130.51 (ArCH), 127.62 (Cq), 127.02 (Cq), 124.86 (ArCH), 123.48 (ArCH), 122.77 (ArCH), 122.72 (ArCH), 122.37 (ArCH), 119.78 (ArCH), 118.78 (ArCH), 111.31 (ArCH), 111.06 (ArCH), 99.94 (C-9b), 76.01 (C-2), 56.69 (C-3), 29.36 (Indole-CH₂); MS (ESI) *m/z* calcd for C₂₅H₁₈ClN₃O₄: 459.09, found 460 [M + H]⁺.

General procedure for the reactions of N-methylation. To a stirred solution of the appropriate tryptophan-derived oxazoloisindolinone (0.32 mmol, 1.0 equiv.) in anhydrous dimethylformamide (2 mL), at 0 °C and under inert atmosphere of nitrogen, sodium hydride (2.0 equiv., dry 95%) was added. After stirring for 30 minutes, methyl iodide (2.0 equiv.) was added and the reaction was slowly allowed to warm up to room temperature for one hour. Ethyl acetate was added (10 mL) to the reaction, and the organic phase washed with water (6 \times 10 mL), with an aqueous saturated solution of NaHCO₃ (10 mL) and then with a brine solution (10 mL). The organic phase was dried over Na₂SO₄. After removal of volatiles under reduced pressure, purification via flash chromatography followed by recrystallization in ethyl acetate/*n*-hexane afforded the desired product.

General procedure for the reactions of N-ethylation. To a stirred solution of the appropriate tryptophan-derived oxazoloisindolinone (0.32 mmol, 1.0 equiv.) in anhydrous dimethylformamide (2 mL), at 0 °C and under inert atmosphere of nitrogen, sodium hydride (2.0 equiv., dry 95%) was added. After stirring for 30 minutes, ethyl iodide (2.0 equiv.) was added and the reaction was slowly allowed to warm up to room temperature till total consumption of the starting material. Ethyl acetate was added (10 mL) to the reaction mixture, and the organic phase washed with deionized water (6 \times 10 mL), with an aqueous saturated solution of NaHCO₃ (10 mL) and then with a brine solution (10 mL). The organic phase was dried over Na₂SO₄. After removal of volatiles under reduced pressure, purification via flash chromatography followed by recrystallization in ethyl acetate/*n*-hexane afforded the desired product.

General procedure for the reactions of N-propylation. To a stirred solution of the tryptophan-derived oxazoloisindolinone (0.32 mmol, 1.0 equiv.) in anhydrous dimethylformamide (3 mL), at 0 °C and under inert atmosphere of nitrogen, sodium hydride (2.0 equiv., dry 95%) was added. After stirring for 30 minutes, propyl bromide (2.0 equiv.) was added and the reaction was slowly allowed to warm up to room temperature till total consumption of the starting material. Ethyl acetate was added (10 mL) to the reaction mixture, and the organic phase washed with deionized water (6 \times 10 mL), with an aqueous saturated solution of NaHCO₃ (10 mL) and then with a brine solution (10 mL). The organic phase was dried over Na₂SO₄. After removal of volatiles under reduced pressure, purification via flash chromatography followed by recrystallization in ethyl acetate/*n*-hexane afforded the desired product.

General procedure for the reactions of N-acetylation. To a stirred solution of the appropriate tryptophan-derived oxazoloisindolinone (0.32 mmol, 1.0 equiv.) in anhydrous dimethylformamide (3 mL) at 0 °C and under inert atmosphere of nitrogen sodium hydride (2.0 equiv., dry 95%) was added. After stirring for 30 minutes, acetic anhydride (2.0 equiv.) was added and the reaction was slowly allowed to warm up to room temperature till total consumption of the starting material. Ethyl acetate was added

(10 mL) to the reaction mixture, and the organic phase washed with water (6 × 10 mL), with an aqueous saturated solution of NaHCO₃ (10 mL) and then with a brine solution (10 mL). The organic phase was dried over Na₂SO₄. After removal of volatiles under reduced pressure, purification via flash chromatography followed by recrystallization in ethyl acetate/*n*-hexane afforded the desired product.

General procedure for the reactions of N-Boc protection. To a solution of the appropriate tryptophanol-derived oxazoloisindolinone lactam (0.13 mmol, 1.0 equiv.) in dry tetrahydrofuran (6 mL) was added dry triethylamine (9 mmol, 2.5 equiv.) and 4-dimethylaminopyridine (0.33 mmol, 0.25 equiv.) under an atmosphere of nitrogen. After 15 minutes of stirring, di-*tert*-butyl bicarbonate (1.7 mmol, 1.25 equiv.) was added and reaction mixture stirred, at room temperature, until consumption of starting material. After reaction completion the mixture was concentrated *in vacuo* and the crude was dissolved in ethyl acetate (20 mL). The organic phase was washed with a saturated solution of NH₄Cl (2 × 15 mL), a saturated solution of NaHCO₃ (2 × 15 mL) and, finally, with brine (1 × 15 mL). The combined organic phases were dried over MgSO₄. After removal of volatiles under reduced pressure, purification via flash chromatography followed by recrystallization in ethyl acetate/*n*-hexane afforded the desired product.

General procedure for the reactions of N-benylation. To a stirred solution of the appropriate tryptophanol-derived oxazoloisindolinone (0.32 mmol, 1.0 equiv.) in anhydrous dimethylformamide (3 mL), at 0 °C and under inert atmosphere of nitrogen, sodium hydride (2.2 equiv., dry 95%) was added. After stirring for 30 minutes, benzyl bromide (1.5 equiv.) was added and the reaction was slowly allowed to warm up to room temperature till total consumption of the starting material. Ethyl acetate was added (10 mL) to the crude of reaction, and the organic phase washed with water (6 × 10 mL), with an aqueous saturated solution of NaHCO₃ (10 mL) and then with a brine solution (10 mL). The organic phase was dried over Na₂SO₄. After removal of volatiles under reduced pressure, purification via flash chromatography followed by recrystallization in ethyl acetate/*n*-hexane afforded the desired product.

General procedure for the reactions of N-benzoylation. To a stirred solution of the appropriate tryptophanol-derived oxazoloisindolinone (0.32 mmol, 1.0 equiv.) in anhydrous dimethylformamide (3 mL), at 0 °C and under inert atmosphere of nitrogen, sodium hydride (2.0 equiv., dry 95%) was added. After stirring for 30 minutes, benzoyl chloride (2.0 equiv.) was added and the reaction was slowly allowed to warm up to room temperature till total consumption of the starting material. Ethyl acetate was added (10 mL) to the crude of reaction, and the organic phase washed with water (6 × 10 mL), with an aqueous saturated solution of NaHCO₃ (10 mL) and then with a brine solution (10 mL). The organic phase was dried over Na₂SO₄. After removal of volatiles under reduced pressure, purification via flash chromatography followed by recrystallization in ethyl acetate/*n*-hexane afforded the desired product.

General procedure for the reactions of N-tosylation. To a stirred solution of the appropriate tryptophanol-derived oxazoloisindolinone (0.32 mmol, 1.0 equiv.) in anhydrous dimethylformamide (3 mL), at 0 °C and under inert atmosphere of nitrogen, sodium hydride (2.0 equiv., dry 95%) was added. After stirring for 30 minutes, *p*-toluenesulfonyl chloride (2.0 equiv.) was added and the reaction was slowly allowed to warm up to room temperature till total consumption of the starting material. Ethyl acetate was added (10 mL) to the crude of reaction, and the organic phase washed with water (6 × 10 mL), with an aqueous saturated solution of NaHCO₃ (10 mL) and then with a brine solution (10 mL). The organic

phase was dried over Na₂SO₄. After removal of volatiles under reduced pressure, purification via flash chromatography followed by recrystallization in ethyl acetate/*n*-hexane afforded the desired product.

Sulforhodamine B (SRB) assay

Cell lines were seeded in 96-well plates at the cells/well density of 5.0 × 10³. Cells were thereafter treated with serial dilutions (1.85–75 μM) of tryptophanol-derived isoindolinones for 24 and 48 h, and its effect on cell proliferation was analysed by SRB assay with the determination of GI₅₀ (concentration that causes 50% of growth inhibition) values. The solvent (DMSO 0.25%) and nutlin-3a (GI₅₀ = 3.2 ± 1.0 μM in HCT116 p53^{+/+} and GI₅₀ = 24.0 ± 0.7 μM in HCT116 p53^{-/-}) were included as controls.

Competitive FP binding assay

The binding affinity of tryptophanol-derived isoindolinones was evaluated by a competitive fluorescence polarization-based (FP-based) binding assay, using a recombinant human His-tagged MDM2 protein (residues 1–118) and a FAM tagged p53-based peptide (5-FAM-βAla-βAla-Phe-Met-Aib-pTyr-(6-Cl-LTrp)-Glu-Ac3c-Leu-Asn-NH₂) as the fluorescent probe. The affinity of this probe compound to MDM2 was determined to be 1.4 ± 0.3 nM by preliminary protein saturation experiments. Mixtures of 5 μl of the tested compound with different concentrations in DMSO and 120 μl of preincubated protein/fluorescent probe complex with fixed concentrations in the assay buffer (100 mM potassium phosphate, pH 7.5, 100 μg/ml bovine γ-globulin, 0.02% sodium azide, with 0.01% Triton X-100) were added into assay plates and incubated at room temperature for 30 minutes with gentle shaking. Final concentrations of the protein and fluorescent probe in the competitive assays were 10 and 1 nM, respectively, and final DMSO concentration was 4%. Negative controls containing protein/fluorescent probe complex only (equivalent to 0% inhibition), and positive controls containing free fluorescent probe only (equivalent to 100% inhibition), were included in each assay plate and utilized to calculate inhibition rates. Fluorescence polarization (mP) values were measured using the Infinite M-1000 plate reader (Tecan U.S., Research Triangle Park, NC) in Microfluor 1 96-well, black, round-bottom plates (Thermo Scientific) at an excitation wavelength of 485 nm and an emission wavelength of 530 nm.^[44]

Molecular docking simulations

The studies were carried out using the crystallographic structure of MDM2 coded by PDB (Protein Data Bank) ID 4WT2 (1.42 Å resolution).^[45] The receptor was prepared with the make_receptor utility of OEDOCKING 3.4.0.2 (from OpenEye Scientific Software, Santa Fe, NM. <http://www.eyesopen.com>), keeping two water molecules (27 and 29) as a part of the receptor. In the case of MDM2, the binding site cavity was detected by molecular probe and its shape potential had an outer contour of 3438 Å balanced between solvent and protein. The small molecules were prepared for docking by means of OpenEye software. In details, ligands were sketched in Picto (version 4.3.0.4), and stored in SMILES format. These structures were transformed in 3D structure with the assigned stereochemistry using OMEGA 3.1.2.2 (OpenEye Scientific Software, Santa Fe, NM. <http://www.eyesopen.com>) and their protonation state was assigned for pH 7.4 using QUACPAC 2.0.2.2 (OpenEye Scientific Software, Santa Fe, NM. <http://www.eyesopen.com>).^[46] Ligand energy minimization was performed with SZYBKI 1.11.0.2 (OpenEye Scientific Software, Santa Fe, NM. <http://www.eyesopen.com>) using the force field MMFF94S, while

conformational analysis was performed with OMEGA 3.1.2.2 with all parameters at their default values and allowing the storage of 400 conformers of each molecule. Molecular docking was performed with the FRED docking program (OEDOCKING 3.4.0.2, OpenEye Scientific Software, Santa Fe, NM. <http://www.eyesopen.com>), using the high docking accuracy settings. In accurate docking simulations, 5 poses of each molecule were stored.^[47,48]

Acknowledgements

This work was supported by National Funds (Fundação para a Ciência e Tecnologia) through iMED.Ulisboa (UIDB/04138/2020), LAQV/REQUIMTE (UIDB/50006/2020), project PTDC/QUI-QOR/29664/2017, Principal Researcher grant CEECIND/01772/2017 (M. M. Santos), and PhD fellowships PD/BD/143126/2019 (V. Barcherini), SFRH/BD/137544/2018 (E. A. Lopes) and SFRH/BD/132341/2017 (D. M. Silva). The authors thank the OpenEye Free Academic Licensing Program for providing a free academic license for molecular modeling and cheminformatics software.

Conflict of Interest

The authors declare no conflict of interest.

Keywords: Cancer · Isoindolinones · MDM2 · p53 · Tryptophanol

- [1] F. Bray, J. Ferlay, I. Soerjomataram, R. L. Siegel, L. A. Torre, A. Jemal, *CA. Cancer J. Clin.* **2018**, *68*, 394–424.
- [2] R. L. Siegel, K. D. Miller, A. Jemal, *CA. Cancer J. Clin.* **2019**, *69*, 7–34.
- [3] L. Cheng, C. Eng, L. Z. Nieman, A. S. Kapadia, X. L. Du, *Am. J. Clin. Oncol. Cancer Clin. Trials* **2011**, *34*, 573–580.
- [4] K. Thanikachalam, G. Khan, *Nutrients* **2019**, *11*, 164–175.
- [5] C. Sawyers, *Nature* **2004**, *432*, 294–297.
- [6] B. Vogelstein, D. Lane, A. J. Levine, *Nature* **2000**, *408*, 307–310.
- [7] K. H. Khoo, K. K. Hoe, C. S. Verma, D. P. Lane, *Nat. Rev. Drug Discov.* **2014**, *13*, 217–26.
- [8] A. C. Joerger, A. R. Fersht, *Annu. Rev. Biochem.* **2016**, *85*, 375–404.
- [9] E. R. Kasthuber, S. W. Lowe, *Cell* **2017**, *170*, 1062–1078.
- [10] X. L. Li, J. Zhou, Z. R. Chen, W. J. Chng, *World J. Gastroenterol.* **2015**, *21*, 84–93.
- [11] M. L. Slattery, L. E. Mullany, R. K. Wolff, L. C. Sakoda, W. S. Samowitz, J. S. Herrick, *Genomics* **2019**, *111*, 762–771.
- [12] K. T. Bieging, *Nat. Rev. Cancer* **2014**, *14*, 359–370.
- [13] J. Chen, *Cold Spring Harb. Perspect. Biol.* **2016**, 1–16.
- [14] K. H. Vousden, K. M. Ryan, *Nat. Rev. Cancer* **2009**, *9*, 691–700.
- [15] L. Galluzzi, G. Pierron, P. Codogno, F. Cecconi, E. Morselli, U. Nannmark, F. Madeo, G. Kroemer, G. Szabadkai, N. Tavernarakis, et al., *Nat. Cell Biol.* **2008**, *10*, 676–687.
- [16] T. Li, N. Kon, L. Jiang, M. Tan, T. Ludwig, Y. Zhao, R. Baer, W. Gu, *Cell* **2012**, *149*, 1269–1283.
- [17] M. Wade, Y. C. Li, G. M. Wahl, *Nat. Rev. Cancer* **2013**, *13*, 83–96.
- [18] P. A. J. Muller, K. H. Vousden, *Cancer Cell* **2014**, *25*, 304–317.
- [19] M. Espadinha, V. Barcherini, E. A. Lopes, M. M. M. Santos, *Curr. Top. Med. Chem.* **2018**, *18*, 647–660.
- [20] X. Liu, R. Wilcken, A. C. Joerger, I. S. Chuckowree, J. Amin, J. Spencer, A. R. Fersht, *Nucleic Acids Res.* **2013**, *41*, 6034–6044.
- [21] M. J. Duffy, N. C. Synnott, J. Crown, *Eur. J. Cancer* **2017**, *83*, 258–265.
- [22] V. J. N. Bykov, S. E. Eriksson, J. Bianchi, K. G. Wiman, *Nat. Rev. Cancer* **2018**, *18*, 89–102.
- [23] E. A. Lopes, S. Gomes, L. Saraiva, M. M. M. Santos, *Curr. Med. Chem.* **2018**, *26*, 7323–7336.
- [24] S. Jeay, S. Ferretti, P. Holzer, J. Fuchs, E. A. Chapeau, M. Wartmann, D. Sterker, V. Romanet, M. Murakami, G. Kerr, et al., *Cancer Res.* **2018**, *78*, 6257–6267.
- [25] M. J. G. W. Ladds, S. Lain, *J. Mol. Cell Biol.* **2019**, *11*, 245–254.
- [26] C. J. A. Ribeiro, J. D. Amaral, C. M. P. Rodrigues, R. Moreira, M. M. M. Santos, *Bioorg. Med. Chem.* **2014**, *22*, 577–584.
- [27] A. Monteiro, L. M. Gonçalves, M. M. M. Santos, *Eur. J. Med. Chem.* **2014**, *79*, 266–272.
- [28] J. Soares, N. A. L. Pereira, A. Monteiro, M. Leão, C. Bessa, D. J. V. A. Dos Santos, L. Raimundo, G. Queiroz, A. Bisio, A. Inga, et al., *Eur. J. Pharm. Sci.* **2015**, *66*, 138–147.
- [29] C. J. A. Ribeiro, J. D. Amaral, C. M. P. Rodrigues, R. Moreira, M. M. M. Santos, *MedChemComm* **2016**, *7*, 420–425.
- [30] J. Soares, L. Raimundo, N. A. L. Pereira, A. Monteiro, S. Gomes, C. Bessa, C. Pereira, G. Queiroz, A. Bisio, J. Fernandes, et al., *Oncotarget* **2015**, *7*, 4326–4343.
- [31] J. Soares, M. Espadinha, L. Raimundo, H. Ramos, A. S. Gomes, S. Gomes, J. B. Loureiro, A. Inga, F. Reis, C. Gomes, et al., *Mol. Oncol.* **2017**, *11*, 612–627.
- [32] S. Gomes, B. Bosco, J. B. Loureiro, H. Ramos, L. Raimundo, J. Soares, N. Nazareth, V. Barcherini, C. Oliveira, A. Bisio, et al., *Cancers* **2019**, *11*, 1151–1171.
- [33] N. A. L. Pereira, A. Monteiro, M. Machado, J. Gut, E. Molins, M. J. Perry, J. Dourado, R. Moreira, P. J. Rosenthal, M. Prudêncio, et al., *ChemMedChem* **2015**, *10*, 2080–2089.
- [34] N. A. L. Pereira, F. X. Sureda, M. Turch, M. Amat, J. Bosch, M. M. M. Santos, *Monatsh. Chem.* **2013**, *144*, 473–477.
- [35] S. S. Batsanov, *Inorg. Mater. Transl. from Neorg. Mater. Orig. Russ. Text* **2001**, *37*, 1031–1–46.
- [36] K. Mierzejewska, M. Bochtler, H. Czapinska, *Nucleic Acids Res.* **2016**, *44*, 485–495.
- [37] I. R. Hardcastle, S. U. Ahmed, H. Atkins, A. H. Calvert, N. J. Curtin, G. Farnie, B. T. Golding, R. J. Griffin, S. Guyenne, C. Hutton, et al., *Bioorg. Med. Chem. Lett.* **2005**, *15*, 1515–1520.
- [38] I. R. Hardcastle, S. U. Ahmed, H. Atkins, G. Farnie, B. T. Golding, R. J. Griffin, S. Guyenne, C. Hutton, P. Källblad, S. J. Kemp, et al., *J. Med. Chem.* **2006**, *49*, 6209–6221.
- [39] A. F. Watson, J. Liu, K. Bennaceur, C. J. Drummond, J. A. Endicott, B. T. Golding, R. J. Griffin, K. Haggerty, X. Lu, J. M. McDonnell, et al., *Bioorg. Med. Chem. Lett.* **2011**, *21*, 5916–5919.
- [40] T. A. Grigoreva, D. S. Novikova, A. V. Petukhov, M. A. Gureev, A. V. Garabadzhiu, G. Melino, N. A. Barlev, V. G. Tribulovich, *Bioorg. Med. Chem. Lett.* **2017**, *27*, 5197–5202.
- [41] I. R. Hardcastle, J. Liu, E. Valeur, A. Watson, U. Ahmed, T. J. Blackburn, K. Bennaceur, W. Clegg, C. Drummond, J. A. Endicott, et al., *J. Med. Chem.* **2011**, *2*, 1233–1243.
- [42] A. S. Gomes, H. Ramos, S. Gomes, J. B. Loureiro, J. Soares, V. Barcherini, P. Monti, G. Fronza, C. Oliveira, L. Domingues, et al., *Biochim. Biophys. Acta Gen. Subj.* **2020**, *1864*, 129440.
- [43] N. A. L. Pereira, F. X. Sureda, M. Pérez, M. Amat, M. M. M. Santos, *Molecules* **2016**, *21*, 1–12.
- [44] Y. Zhao, S. Yu, W. Sun, L. Liu, J. Lu, D. McEachern, S. Shargary, D. Bernard, X. Li, T. Zhao, et al., *J. Med. Chem.* **2013**, *56*, 5553–5561.
- [45] Y. Rew, D. Sun, X. Yan, H. P. Beck, J. Canon, A. Chen, J. Duquette, J. Eksterowicz, B. M. Fox, J. Fu, et al., *J. Med. Chem.* **2014**, *57*, 10499–10511.
- [46] P. C. D. Hawkins, A. G. Skillman, G. L. Warren, B. A. Ellingson, M. T. Stahl, *J. Chem. Inf. Model.* **2010**, *50*, 572–584.
- [47] M. McGann, *J. Chem. Inf. Model.* **2011**, *51*, 578–596.
- [48] M. McGann, *J. Comput.-Aided Mol. Des.* **2012**, *26*, 897–906.

Manuscript received: July 15, 2020
 Accepted manuscript online: July 31, 2020
 Version of record online: September 2, 2020